Leader-follower formation control of nonholonomic wheeled mobile robots using only position measurements

Hasan A Poonawala, Aykut C Satici and Mark W Spong

***Abstract*—This paper deals with the formation control problem for a team of nonholonomic wheeled mobile robots. Each robot has a leader robot with respect to which a constant relative position is to be maintained, except for a single robot which defines the motion of the formation. We present a feedback control method that guarantees convergence of the relative position of any follower robot (with respect to its leader) to desired values. The controller does not require sensing of the leader's velocity. Instead, an adaptive method is used to estimate the leader's forward velocity.The resulting closed loop system is shown to be semi-globally asymptotically stable. Simulation results are presented in order to demonstrate the performance of the controller for two robots, and a team of mobile robots.**

I. Introduction

Multi-robot systems present a more robust and cheaper solution to certain tasks that are better performed using several low-cost robots rather than single, complex ones. A multi-robot system may be required to travel over large distances in order to reach a site related to a mission or task. While traversing the distances, it may be desirable for the robots to move in a rigid formation with fixed inter-robot distances. This gives rise to the formation control problem. Further, it is often desired that the control of these distances be done in a decentralized manner, rather than through a common supervisor or command center. Such control solutions can be applied to military maneuvers or automated highways.

Several approaches to formation control have been presented. The methods of formation control commonly employed can be classified into leader-follower methods [1]–[3], behavior-based control [4]–[6], [10], variable structure control techniques [7], and consensus based methods [8], [9]. The behavior-based control methods provide the robots with actions in reaction to sensor data. A formation emerges from the local interactions occurring throughout the team. This behavior is often encoded using potential functions. The leader-follower methods use techniques such as input-output partial feedback linearization of the dynamics of the relative pose between two robots [2]. Another leader-follower method makes use of potential functions and virtual leaders [1]. Consensus based methods account for the effect of the information flow between agents on the stability and performance of formation control while designing the control law.

The linearization in [2] requires knowledge of the leader velocity, however sensing velocity is difficult and differentiating position to obtain velocity is too noisy. To prevent facing these issues, an extended Kalman filter (EKF) is then proposed for obtaining the leader velocity. It is unclear whether this choice is made to account for noisy measurements, or that such a filter is required to estimate the velocities even in the absence of noise. Either way the convergence analysis assumes that the filter output has converged to the true values, whereas there are no results guaranteeing the convergence of the EKF.

Instead of using a Kalman filter, one could use a dynamic estimator to obtain the leader velocity information. This approach has been taken in [3], [6], [10]. The work in [6], [10] use artificial potential functions, which do not guarantee a particular relative position unless each robot follows two other robots. The work in this paper is similar to that in [3]. The forward and angular velocities are adapted and used in a feedback control law which guarantees ultimate boundedness of the errors in position, for arbitrary but bounded leader velocity. In the case of straight line motion of the leader, the errors are shown to converge to zero.

The work in this paper is a progression from the work in [11]. The choice of leader-follower methods is practical when using a vision-based measurement system, since then each robot must sense the relative pose information of only one robot. A feedback control law was proposed which did not use velocity information of the leader, and the resulting errors in relative position are shown to be uniformly ultimately bounded. Note that the leader velocity was assumed to be bounded, but not necessarily constant. The error bound could be arbitrarily reduced by increasing the control gains, similar to [3], but without requiring any estimation of the leader velocity. A significant feature of the work in [11] was that it was very simple to implement with high reliability and low computational effort compared to other methods.

The controller we present also uses an adaptation-like method to estimate the leader forward velocity. Since [11] achieves ultimately bounded errors without adaptation, we focus on the case where the leader moves in a straight line or a circle, where the estimation actually yields an advantage. Our work shows that estimation of the angular velocity is unnecessary for convergence of the relative position to their desired values. Also, it is clear that our method is much simpler to implement, especially when using the measurement system in [11] which directly provides ρ, ψ and γ.

In the next section we introduce some background relevant

Hasan A Poonawala and Aykut C Satici are PhD students at the Erik Jonsson School of Engineering and Computer Science, University of Texas at Dallas, Richardson, Texas, USA {hasanp,acsatici}@utdallas.edu

Mark W Spong is the Dean of the Erik Jonsson School of Engineering and Computer Science, University of Texas at Dallas, Richardson, Texas, USA mspong@utdallas.edu

This research was partially supported by the National Science Foundation Grants ECCS 07-25433 and CMMI-0856368, by the University of Texas STARs program, and by DGIST R&D Program of the Ministry of Education, Science and Technology of Korea(12-BD-0101).

978-1-4673-5769-2/13/$31.00 ©2013 IEEE

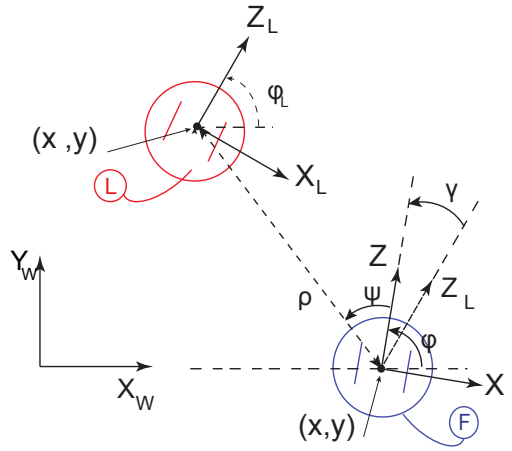

Fig. 1: WMRs in inertial and relative coordinates

to the problem. We present the controller, and prove convergence of the relative position states to their desired values. We then present simulation results to demonstrate the performance of the controller, and conclude with a discussion about the controller.

II. Background

A. Differential-drive Wheeled Mobile Robot

Differential drive wheeled mobile robots (WMR) are popular for their low cost and simplicity, and we base our work on implementation on such robots. In an inertial world reference frame, the configuration of a WMR is given by the position of the center between its two wheels (x,y) and the angle ϕ of its heading direction. The heading direction is the line perpendicular to the axes of wheel rotations, and is positive in the direction of forward motion (See Fig. 1). The kinematic equations of motion of a WMR are

$$\begin{bmatrix}\dot{x}\\ \dot{y}\\ \dot{\phi}\end{bmatrix} = \begin{bmatrix}\cos\phi & 0\\ \sin\phi & 0\\ 0 & 1\end{bmatrix}\begin{bmatrix}v\\ \omega\end{bmatrix} \tag{1}$$

where v and ω are the forward speed and angular velocity of the WMR. Assume robot L with configuration (x_L,y_L,ϕ_L) has a Cartesian frame attached to it (Fig. 1). The z-axis coincides with the robot's heading direction, the y-axis (not shown in Fig. 1) is normal to the ground plane oriented downwards, and the x-axis is chosen to result in a right-handed Cartesian frame. This convention for the robot frame axes comes from the convention for a frame fixed on a camera, as used in [11].

B. Relative kinematics between two WMR

Let the configurations of the leader and follower robots in the world frame be (x_L,y_L,ϕ_L) and (x,y,ϕ) respectively. In the frame of the follower, the polar coordinates of the leader are given by (ρ, ψ). The angle that the z-axis of the leader frame makes with the z-axis of the follower is given by γ (see Fig. 1). The relative coordinates of the leader in the frame of the follower robot are then

$$\begin{bmatrix}\rho\\ \psi\\ \gamma\end{bmatrix} = \begin{bmatrix}\left((x_L-x)^2+(y_L-y)^2\right)^{\frac{1}{2}}\\ \arctan\left(\frac{y_L-y}{x_L-x}\right)-\phi\\ \phi_L-\phi\end{bmatrix} \tag{2}$$

Using (1) and differentiating (2) results in

$$\dot{\rho} = -v\cos\psi + v_L\cos(\gamma-\psi) \tag{3a}$$

$$\dot{\psi} = v\frac{\sin\psi}{\rho} - \omega + v_L\frac{\sin(\gamma-\psi)}{\rho} \tag{3b}$$

$$\dot{\gamma} = \omega_L - \omega \tag{3c}$$

where v_L and ω_L are translational and angular velocities of the leader WMR, v and ω are translational and angular velocities of the follower WMR, respectively.

III. Control Design

The control goal is to regulate the relative position between the follower and the leader WMRs, where the leader moves with constant positive translational and angular velocity $(v_L,\omega_L) \in \mathbb{R}_+ \times \mathbb{R}$. This amounts to keeping (ρ,ψ) at a desired value (ρ_d,ψ_d), cf. Fig. 1. The non-holonomic kinematics makes it impossible to control γ in addition to ψ and γ through smooth feedback. In any case, controlling the steady state value of γ is not required for formation control.

The following control linearizes the dynamics of the variables (ρ,ψ):

$$v = \frac{v_L\cos(\gamma-\psi)}{\cos\psi} + \bar{v} \tag{4a}$$

$$\omega = \frac{v_L\sin(\gamma-\psi)}{\rho} + \frac{v\sin(\psi)}{\rho} + \bar{\omega} \tag{4b}$$

resulting in the dynamics

$$\dot{\rho} = \bar{v} \tag{5a}$$

$$\dot{\psi} = \bar{\omega} \tag{5b}$$

This is the same control used in [2], which requires exact knowledge of the leader's forward velocity v_L.

Since we do not measure v_L, we augment the system in (3) with a single state σ, which acts as an estimator for v_L. The dynamics for this state are chosen as

$$\dot{\sigma} = \frac{K_\sigma}{4}\cos(\gamma-\psi)\tilde{\rho} \tag{6}$$

The control is then selected as

$$v = \frac{\sigma\cos(\gamma-\psi)+\bar{K}_v\tilde{\rho}}{\cos\psi} \tag{7a}$$

$$\omega = \frac{\sigma\sin(\gamma-\psi)}{\rho} + \frac{v\sin(\psi)}{\rho} + \bar{K}_\omega\tilde{\psi} \tag{7b}$$

where $\tilde{\rho} = (\rho-\rho_d)$ and $\tilde{\psi} = (\psi-\psi_d)$. Let $\tilde{\sigma} = (\sigma - v_L)$. The closed loop kinematics can now be written as

$$\dot{\rho} = -\bar{K}_v\tilde{\rho} - \cos(\gamma-\psi)\tilde{\sigma} \tag{8a}$$

$$\dot{\psi} = -\bar{K}_\omega\tilde{\psi} + \frac{\sin(\gamma-\psi)}{\rho}\tilde{\sigma} \tag{8b}$$

$$\dot{\gamma} = \omega_L - \bar{K}_\omega\tilde{\psi} - \frac{\sigma\sin\gamma}{\rho\cos\psi} - \bar{K}_v\frac{\sin\psi}{\rho}\tilde{\rho} \tag{8c}$$

$$\dot{\sigma} = \frac{K_\sigma}{4}\cos(\gamma-\psi)\tilde{\rho} \tag{8d}$$

Let the state be denoted by $q = \begin{bmatrix}\rho & \psi & \gamma & \sigma\end{bmatrix}^T \in \mathcal{Q} = \mathbb{R}_{>0}\times\mathcal{S}^1\times\mathcal{S}^1\times\mathbb{R}$. We define a domain D as

$$D := \{q\in\mathcal{Q} \mid |\psi| < \pi/2\} \tag{9}$$

The analysis of the closed loop kinematics is done in four steps. First we characterize the equilibrium points of the system, deriving a condition that ensures a unique equilibrium state exists. We then analyze the dynamics of the relative distance ρ, relative polar angle ψ and estimate σ, and show that they asymptotically converge to their equilibrium values from any initial condition in D. The orientation γ is then shown to converge to it's equilibrium value. We then state the main theorem showing that the equilibrium is asymptotically stable on D.

Proposition III.1. *If $\rho_d \neq \left|\frac{v_L}{\omega_L}\right|$ and $\frac{|\omega_L|\rho_d \cos\psi_d}{v_L} \leq 1$ then the closed loop system described by* (8) *has a unique equilibrium q_e given by*

$$q_e = \begin{bmatrix} \rho_d & \psi_d & \arcsin\left(\frac{\omega_L \rho_d \cos\psi_d}{v_L}\right) & v_L \end{bmatrix}^T \qquad (10)$$

Proof: See Appendix A-A ∎

A consequence of Proposition III.1 is that if $\rho_d \neq \left|\frac{v_L}{\omega_L}\right|$ then $\cos(\gamma - \psi) \not\equiv 0$. For the remainder of this section we assume that Proposition III.1 holds.

We consider a subsystem of the dynamics in (8)

$$\dot{\rho} = -K_v \tilde{\rho} - \cos(\gamma - \psi)\ \tilde{\sigma} \qquad (11a)$$

$$\dot{\sigma} = \frac{K_\sigma \cos(\gamma - \psi)}{4}\tilde{\rho} \qquad (11b)$$

$$\dot{\psi} = -\bar{K}_\omega \tilde{\psi} + \frac{\sin(\gamma - \psi)}{\rho}\tilde{\sigma} \qquad (11c)$$

We define the function $V_1(\tilde{\rho}, \tilde{\sigma})$ as

$$V_1(\tilde{\rho}, \tilde{\sigma}) = \frac{1}{2}\tilde{\rho}^2 + \frac{4}{K_\sigma}\tilde{\sigma}^2 \qquad (12)$$

Let $\bar{q} \in \bar{\mathcal{Q}}$, where $\bar{q} = (\rho, \psi, \sigma)$ and $\bar{\mathcal{Q}} = \mathbb{R}_{>0} \times \mathcal{S}^1 \times \mathbb{R}$. We define the set $\bar{D}$ as

$$\bar{D} := \{q \in \mathcal{Q} \mid |\psi| < \pi/2\} \qquad (13)$$

Let the initial condition at $t = t_0$ be $\bar{q}_0 = (\rho(t_0), \psi(t_0), \sigma(t_0))$ and $V_{10} = V_1(\rho(t_0) - \rho_d, \sigma(t_0) - v_L)$ We define the compact sets $U(\bar{q}_0)$ and $W(\bar{q}_0)$ as

$$U(\bar{q}_0) := \{(\rho, \sigma) \in \mathbb{R}_{>0} \times \mathbb{R} | V_1(\tilde{\rho}, \tilde{\sigma}) \leq V_{10} \text{ and } \rho \geq \rho_{min}\} \qquad (14a)$$

$$W(\bar{q}_0) := \{\bar{q} \in \bar{\mathcal{Q}} | (\rho, \sigma) \in U(\bar{q}_0) \text{ and } |\psi| \leq (\pi/2 - \epsilon)\} \qquad (14b)$$

where $\epsilon > 0$ and ρ_{min} are design parameters.

Lemma III.1. *Assume that $\rho_d > 0$, $|\psi_d| < \pi/2$ and that there exists v_{max} such that $0 < v_L < v_{max}$. For any initial condition $\bar{q}_0 \in \bar{D}$, there exist appropriate gains in* (6) *and* (7) *and paramters $\epsilon > 0$ and ρ_{min} such that the solution $\bar{q}(t, \bar{q}_0)$ of the closed loop system* (11) *remains in $W(\bar{q}_0)$ $\forall t \geq t_0$*

Proof: See Appendix A-B ∎

Lemma III.1 guarantees that $\psi(t) \neq \pi/2$ and $\sigma(t) < \infty$ $\forall t \geq t_0$. We now show that ρ and σ converge to their equilibrium values.

Lemma III.2. *Assume that Lemma III.1 holds, then the equilibrium (ρ_d, v_L) of the subsystem given by equations* (11a) *and* (11b) *is asymptotically stable.*

Proof: See Appendix A-C ∎

This now enables us to guarantee that $\psi(t) \to \psi_d$.

Lemma III.3. *Assume that Lemma III.2 holds. Then $\psi(t) \to \psi_d$.*

Proof: See Appendix A-D ∎

Finally, the dynamics for γ are rewritten as

$$\begin{aligned} \dot{\gamma} &= \omega_L - \bar{K}_\omega \tilde{\psi} - \frac{\sigma \sin(\gamma)}{\rho \cos\psi} - \frac{K_v \tilde{\rho} \sin\psi}{\rho} \\ &= \omega_L - \frac{v_L \sin(\gamma)}{\rho \cos\psi} - g(\tilde{\rho}, \tilde{\psi}, \tilde{\sigma}, \gamma) \end{aligned} \qquad (15)$$

where

$$g(\tilde{\rho}, \tilde{\psi}, \tilde{\sigma}, \gamma) = \bar{K}_\omega \tilde{\psi} + \frac{\tilde{\sigma} \sin(\gamma)}{\rho \cos\psi} + \frac{K_v \tilde{\rho} \sin\psi}{\rho} \qquad (16)$$

and $g(0, 0, 0, \gamma) = 0$. We use this fact to show that γ reaches its equilibrium value.

Lemma III.4. *Assume that Proposition III.1, Lemma III.2 and Lemma III.3 hold. Then $\gamma \to \arcsin\frac{|\omega_L|\rho_d \cos\psi_d}{v_L}$ as $t \to \infty$*

Proof: See Appendix A-E ∎

We are now in a position to state the main result.

Theorem III.5. *If the following conditions hold*

C1. $v_L \neq \rho_d |\omega_L|$ *and* $\frac{|\omega_L|\rho_d \cos\psi_d}{v_L} \leq 1$
C2. $v_L < v_{max}$
C3. $\psi_d < \pi/2$ *and* $\rho_d > 0$
C4. $K_\sigma > 0$, $\bar{K}_v$ *and* $\bar{K}_\omega$ *are designed as in Lemma III.1*

Then the equilibrium of (8) *is semi-globally asymptotically stable.*

Proof: See Appendix A-F ∎

Remark 1. These results can be extended to the case where $\dot{v}_L \in L_2$ and $\dot{\omega}_L \in L_2$. This implies that the leader acceleration is bounded and its motion asymptotically approaches a straight line or circle as $t \to \infty$. The directional derivatives of the candidate Lyapunov functions will contain additional terms that are linear in $\dot{v}_L$ and $\dot{\omega_L}$. These terms can be dominated by appropriate selection of gains K_v and they vanish as $t \to \infty$. Thus the same arguments will be valid. This allows for a richer class of leader motions to be used.

IV. Simulation Results

We present separate simulations to demonstrate the properties of the control developed in Section III. We consider the following cases

S1 The leader moves in a straight line
S2 The leader moves in a circle
S3 Four robots follow a leader in formation

In all the simulations, the following parameters are used: $\rho_{min} = 7$m, $\epsilon = \pi/12$rad, $v_L = 4$m/s, and $v_{max} = 5$m/s. The gains are designed as in Lemma III.1, taking the minimum allowable gains. This yields $K_v = 1.666667$ and $K_\omega = 1.364185$. The estimator gain is $K_\sigma = 4.5$. The initial conditions for each simulation are given in Table I.

TABLE I: Initial conditions for simulations

Parameter	S1	S2	S3
$\rho(0)$ [m]	12.0	12.0	-
$\psi(0)$ [rad]	0.785	0.523599	0
$\gamma(0)$ [rad]	-0.262	-0.261799	0
$\sigma(0)$ [m/s]	0	0	0
ρ_d [m]	10.0	10.0	10.0
ψ_d [rad]	0	0.785398	$\pm$ 0.785398
ω_L [rad/s]	0	0.3	0.05

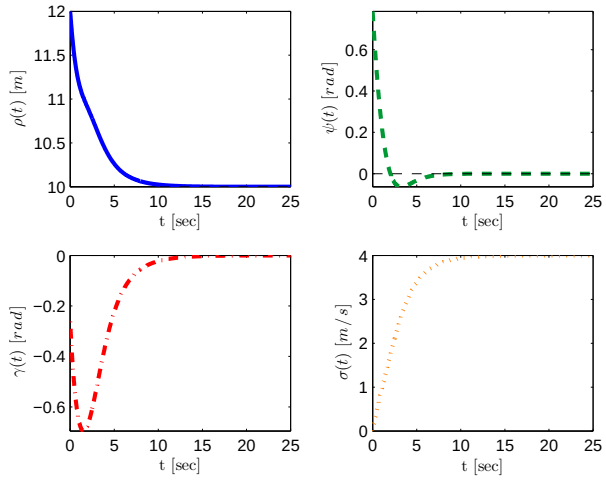

Fig. 2: Simulation results for S1. The states converge asymptotically to the equilibrium condition indicated by the black dashed line

Figure 2 shows the result of the simulation S1. We see that the states converge to their equilibrium values. As expected, the equilibrium value of γ when the leader moves in a straight line is 0rad. The maximum control efforts during the motion are $\max\ |v|= 4.71$m/s and $\max\ |w|= 0.71$rad/s.

For the simulation S2, the leader moves in a circular path. The results are seen in figure 3. Once again the states converge to their equilibrium values. The maximum control efforts during the motion are $\max\ |v|= 5.63$m/s and $\max\ |w|= 0.3$rad/s.

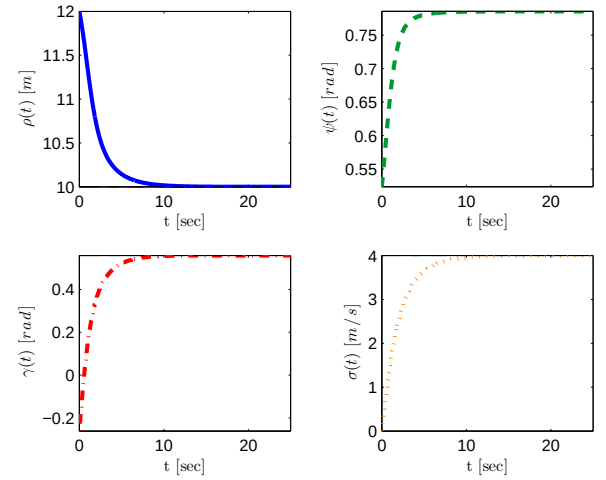

Fig. 3: Simulation results for S2. The states converge asymptotically to the equilibrium condition indicated by the black dashed line.

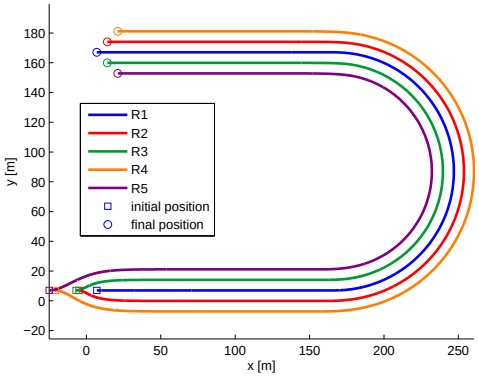

Fig. 4: Simulation results for S3: Paths in $\mathbb{R}^2$

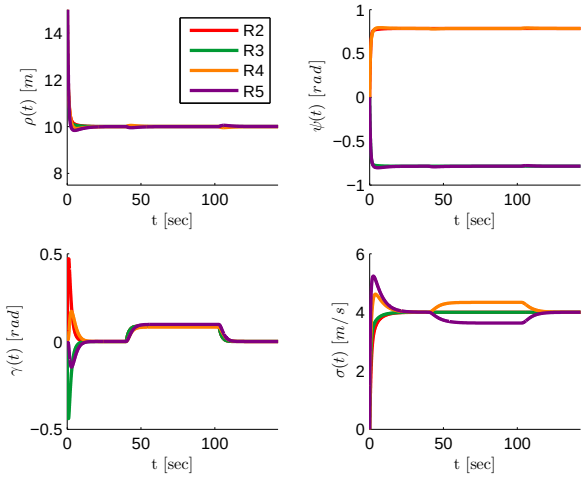

Fig. 5: Simulation results for S6: The relative coordinates for the follower robots $R2 - R5$. The relative positions converge to their desired values during each phase of leader motion

In the simulation $S3$, $R1 - R5$ are five robots which must move in a 'vee' formation. the leader $R1$ moves with $v_L = 4$m/s. The leader's path consists of two linear sections and one semicircle where $\omega_L = 0.1$rad/s. Robots $R2$ and $R3$ follow $R1$. In turn, $R4$ follows $R2$ and $R5$ follows $R3$. We see that the relative positions of all the robots converge to their desired values whether $R1$'s motion is linear or circular. During the circular motion, the forward velocity of each robot depends on the radius of curvature of the robot path. This results in different values of σ for the follower robots. Note that the controller smoothly handles the change in the leader motion. In all three simulations, $|\psi(t)| < (\pi/2 - \epsilon)$ and $\rho(t) > \rho_{min}$, showing that the controller meets the design specification.

V. Conclusion

We have developed a controller for the purpose of regulating the relative position between two robots, when the leader robot moves with a constant velocity. As mentioned in [2], several optimal trajectories and path planning algorithms consist of sequences of constant velocity motions. The follower robot

only has relative pose information available to it, and the controller accounts for this by estimating the leader velocity. We show that the closed loop system converges to the desired equilibrium value for any valid initial condition, both through analysis and simulation.

The controller presented has some advantages over the controllers in [2], [11]. Unlike [11], the errors in relative position converge to zero. When compared to the estimator in [2], [3], ours consists of a single state, with only one gain to be tuned. The estimator is also shown to converge, while the convergence of that in [2] has not been analyzed. We claim that our formation control method is the simplest to implement, especially with the measurement system [11].

The future work consists of implementing this controller on a setup similar to that in [11]. The design parameter ϵ is useful in guaranteeing that the leader stays within the field of view of the follower robot's camera.

APPENDIX A

A. Proof of Proposition III.1

Assume that $\cos(\gamma_e - \psi_e) \neq 0$, where subscript e denotes the equilibrium value. Setting the LHS of (8) to zero, it can then seen that $\tilde{\rho}, \tilde{\psi}, \tilde{\sigma} = 0$ uniquely determines the equilibrium values for ρ,ψ and σ respectively. Setting $\dot{\gamma} = 0$ in (8c) yields

$$\begin{aligned} \gamma_e &= \arcsin\left(\frac{\omega_L \rho_e \cos\psi_e}{v_L}\right) \\ &= \arcsin\left(\frac{\omega_L \rho_d \cos\psi_d}{v_L}\right) \end{aligned} \tag{17}$$

which exists since we assume that $\frac{|\omega_L|\rho_d \cos\psi_d}{v_L} \leq 1$. Thus

$$q_e = \begin{bmatrix} \rho_d & \psi_d & \arcsin\left(\frac{\omega_L \rho_d \cos\psi_d}{v_L}\right) & v_L \end{bmatrix}^T \tag{18}$$

is a valid equilibrium of (8) when $\cos(\gamma_e - \psi_e) \neq 0$.

Now we assume that $\cos(\gamma_e - \psi_e) = 0$. This yields $\dot{\sigma} = 0$ in (8d). From (8a) we then derive that $\dot{\rho} = 0 \Rightarrow \rho_e = \rho_d$. Equations (8b) and (8c) can be rewritten as

$$0 = -K_\omega(\psi - \psi_d) - \sin(\gamma_e - \psi_e)\frac{v_L - \sigma_e}{\rho_d} \tag{19a}$$

$$0 = \omega_L - \sin(\gamma_e - \psi_e)\frac{\sigma_e}{\rho_d} - K_\omega(\psi_e - \psi_d) \tag{19b}$$

which yield

$$\omega_L = \pm\frac{v_L}{\rho_d} = \pm\frac{\sigma_e}{\rho_d} + K_\omega(\psi_e - \psi_d) \tag{20}$$

which yield infinite solutions for σ_e and ψ_e. However, ensuring that $\rho_d \neq \left|\frac{v_L}{\omega_L}\right|$ precludes the existence of this solution, and q_e is the only possible equilibrium point of (8).

B. Proof of Lemma III.1

The right hand side of (11) is Lipschitz on $\bar{D}$. Theorem 3.1 in [12] allows us to conclude that a unique solution $\bar{q}(t, \bar{q}_0)$ exists for $t \in [t_0, t_0 + \delta]$. Due to continuity, there must be some $0 < \delta' \leq \delta$ for which $\psi(t) \neq \pi/2$ and $\sigma(t) < \infty$ for $t \in [t_0, t_0 + \delta']$. We now design the gains and parameters in (6), (7) and (14) so that $\bar{q}(t_0 + \delta') \in W(\bar{q}_0)$. We note that V_1 in (12) is positive definite if $\bar{K}_v > 0$ and $K_\sigma > 0$, and that $V_1 \leq c$ for some constant $c < \infty$ defines compact sets in (ρ, σ). We find $\dot{V}_1$ along solutions of (11).

$$\begin{aligned} \dot{V}_1 &= \tilde{\rho}\dot{\rho} + \frac{2}{K_\sigma}(\sigma - v_L)\dot{\sigma} \\ &= \tilde{\rho}(-\bar{K}_v\tilde{\rho} - \cos(\gamma - \psi)\tilde{\sigma} + \frac{4}{K_\sigma}\tilde{\sigma}\frac{K_\sigma}{4}\cos(\gamma - \psi)\tilde{\rho} \\ &= -\bar{K}_v\tilde{\rho}^2 \end{aligned} \tag{21}$$

which is clearly negative semi-definite on $[t_0, t_0 + \delta'] \times \bar{D}$ if $\bar{K}_v > 0$. Thus $(\rho, \sigma) \in U'\ \forall t \in [t_0, t_0 + \delta']$, where $U' = \{(\rho, \sigma) \in \mathbb{R}_{>0} \times \mathbb{R} | V(\rho, \sigma) \leq V_{10}\}$. In order to have that $(\rho, \sigma) \in U\ \forall t \in [t_0, t_0 + \delta']$, we must show that $\rho(t) \geq \rho_{min}$.

To achieve this, the condition that $\dot{\rho} > 0$ when $\rho(t) = \rho_{min}$ must hold. We can choose ρ_{min} to satisfy$0 < \rho_{min} < \min\{\rho(0), \rho_d\}$, which exists since $\rho(0) > 0$ and $\rho_d > 0$ by assumption. From (11a) we obtain the condition

$$\begin{aligned} &-\bar{K}_v(\rho_{min} - \rho_d) - \cos(\gamma - \psi)(\sigma - v_L) > 0 \\ &\Rightarrow \bar{K}_v(\rho_d - \rho_{min}) > \cos(\gamma - \psi)(\sigma - v_L) \end{aligned} \tag{22}$$

However we can bound the right hand side of (22) as

$$\begin{aligned} \cos(\gamma - \psi)(\sigma - v_L) &\leq (v_L + |\sigma|) \\ &< (v_{max} + |\sigma|) \end{aligned} \tag{23}$$

so that (22) is satisfied when the following condition is satisfied:

$$\bar{K}_v(\rho_d - \rho_{min}) > (v_L + |\sigma|) \tag{24}$$

we now choose $\bar{K}_v$ as

$$\bar{K}_v(\sigma) = K_v + \frac{\sigma}{\rho_d - \rho_{min}} \tag{25}$$

Inequality (24) reduces to

$$K_v > \frac{v_L}{\rho_d - \rho_{min}} \tag{26}$$

Hence, we choose K_v as

$$K_v \geq \frac{v_{max}}{\rho_d - \rho_{min}} > \frac{v_L}{\rho_d - \rho_{min}} \tag{27}$$

and the resulting choice of gain $\bar{K}_v(\sigma)$ clearly satisfies (24), in turn it satisfies (22). Since $(\rho, \sigma) \in U'\ \forall t \in [t_0, t_0 + \delta']$, $\sigma(t)$ is clearly bounded, and the control effort is also bounded. Thus this gain ensures that $\rho(t) \geq \rho_{min} \forall t \in [t_0, t_0 + \delta']$.

We must finally ensure that $\psi(t)$ cannot approach $\pi/2$. We do this by ensuring that for large enough $|\psi|$, $\dot{V}_2 < 0$. We select $\epsilon > 0$ to satisfy $\max\{|\psi_d|, |\psi(0)|\} < \epsilon < \pi/2$ which exists by assumption. We now require that $\dot{\psi} < 0$ when $\psi = (\pi/2 - \epsilon)$ and that $\dot{\psi} > 0$ when $\psi = -(\pi/2 - \epsilon)$. From (11c) this condition is satisfied when

$$\bar{K}_\omega(\pi/2 - \epsilon - |\psi_d|) > |(v_L - \sigma)|\frac{|\sin(\gamma - \psi)|}{\rho} \tag{28}$$

The term on the right hand side of the inequality above can be bounded as

$$(v_L - \sigma)|\frac{|\sin(\gamma - \psi)|}{\rho}| \leq \frac{v_L + |\sigma|}{\rho_{min}} < \frac{v_L + |\sigma|}{\rho_{min}} \tag{29}$$

We now choose $\bar{K}_\omega$ as

$$\bar{K}_\omega = K_\omega + \frac{|\sigma|}{\rho_{min}(\frac{\pi}{2} - \epsilon - |\psi_d|)} \tag{30}$$

Due to (29) we satisfy (28) if

$$\begin{aligned} \bar{K}_\omega(\pi/2-\epsilon-\psi_d) &> \frac{(v_L+|\sigma|)}{\rho_{min}} \\ \Rightarrow K_\omega &\geq \frac{v_{max}}{\rho_{min}(\pi/2-\epsilon-|\psi_d|)} \end{aligned} \tag{31}$$

Thus we guarantee that $|\psi(t)| \leq (\pi/2-\epsilon)\ \forall t \in [t_0, t_0+\delta']$ for a suitable choice of K_ω. The preceding discussion shows that for the finite time interval $[t_0, t_0+\delta']$ the solution $\bar{q}(t, \bar{q}_0)$ cannot cross the boundary of $W(\bar{q}_0)$ denoted as $\partial W(\bar{q}_0)$, rendering $W(\bar{q}_0)$ positively invariant. We repeat the above argument at $t = t_0 + \delta'$ using the Lipschitz property of the dynamics (11) on $W(\bar{q}_0) \subset \bar{D}$ and can thus extend the interval for which the solution $q(t, \bar{q}_0) \in W(\bar{q}_0)$ arbitrarily, completing the proof.

C. Proof of Lemma III.2

The function in (12) is taken as a candidate lyapunov function V_1. It is positive definite for positive gains $\bar{K}_v$ and K_σ, with$V_1(\tilde{\rho}, \tilde{\sigma}) = 0$. Its derivative along solutions of (11a) and (11b) is given in (21).

The condition that $\psi(t) \neq \pm\pi/2\ \forall t \geq t_0$ ensures that the control remains bounded so that the closed loop equations (11a) and (11b) are valid. Clearly $\dot{V}_1 \leq 0$ on D (from (21)). We invoke La Salle's Invariance Principle [12] and observe that the set where $\dot{V}_1 \equiv 0$ is given by the solution $\rho \equiv \rho_d$. Since $\rho_d \neq \left|\frac{v_L}{\omega_L}\right|$ we have that $\cos(\gamma - \psi) \not\equiv 0$. From (11a) in order that $\dot{\rho} \equiv 0$ we must have that $\sigma \equiv v_L$. Thus the largest invariant set of the Lyapunov function V_1 consists of the point $(\tilde{\rho}, \tilde{\sigma}) = 0$. We conclude that the equilibrium of (11a) and (11b) is asymptotically stable.

D. Proof of Lemma III.3

The candidate Lyapunov function $V_2(\tilde{\psi}) = \frac{1}{2}\tilde{\psi}^2$ is proposed where $V_2(\tilde{\psi}) > 0$ when $\psi \neq \psi_d$ and $V_2(0) - 0$. The derivative along the solutions of $\psi(t)$ is given by

$$\begin{aligned} \dot{V}_2 &= \tilde{\psi}\dot{\psi} = \tilde{\psi}\left(-\bar{K}_\omega(\sigma)\tilde{\psi} + \frac{\sin(\gamma-\psi)}{\rho}(v_L - \sigma)\right) \\ &= -\bar{K}_\omega(\sigma)\tilde{\psi}^2 - \frac{\sin(\gamma-\psi)}{\rho}(v_L-\sigma)\tilde{\psi} \end{aligned} \tag{32}$$

For ψ such that $(\psi - \psi_d) \geq (\pi/2 - \epsilon - |\psi_d|)$ we know that $\dot{V}_2 < 0$, from Lemma III.1. Thus when $\sigma(t) \neq v_L$ the term $\tilde{\psi}$ is ultimately bounded. From Lemma III.1 we know that Lemma III.2 holds, so that $\sigma \to v_L$ as $t \to \infty$. Thus as $t \to \infty$, $\dot{V}_2 < 0$ holds $\forall \psi \neq \psi_d$, that is, the region of ultimate boundedness shrinks to the set $\psi = \psi_d$. Hence, $\psi \to \psi_d$ asymptotically.

E. Proof of Lemma III.4

Let $y = \sin\gamma - \frac{\omega_L \rho_d \cos\psi_d}{v_L}$ and $V_y = y^2/2$ be a candidate Lyapunov function. Then

$$\begin{aligned} \dot{V}_y &= y\dot{y} = y\cos\gamma\dot{\gamma} \\ &= y\sqrt{1-y^2}\left(\omega_L - \frac{v_L\sin(\gamma)}{\rho_d\cos\psi_d} - g(\tilde{\rho},\tilde{\psi},\tilde{\sigma},\gamma)\right) \\ &= -\sqrt{1-y^2}(y^2 + yg(\tilde{\rho},\tilde{\psi},\tilde{\sigma},\gamma)\frac{\rho_d\cos\psi_d}{v_L})\frac{v_L}{\rho_d\cos\psi_d} \end{aligned} \tag{33}$$

Clearly $\dot{V}_y < 0$ when $|y| > |g|\frac{\rho_d\cos\psi_d}{v_L}$ and $y \neq \pm 1$. Since we assume Proposition III.1 holds, $y = 0$ is a unique equilibrium of 8, and we rule out $y^2 \equiv 1$. From Lemmas III.2 and III.3 we know that $|g| \to 0$, since $\bar{q} \to \bar{q}_e$ and $g(0,0,0,\gamma) = 0$. Hence for large enough t, y is ultimately bounded, and the region of ultimate boundedness reduces to the set $y = 0$ as $t \to \infty$. Thus $\gamma \to \arcsin\frac{|\omega_L|\rho_d\cos\psi_d}{v_L}$ as $t \to \infty$.

F. Proof of Theorem III.5

The condition $C1$ guarantees that an equilibrium of (8) exists and is unique, from Proposition III.1. Conditions $C2$ and $C3$ satisfies the conditions for Lemma III.1. We can then choose appropriate values for the gains in $C4$ such that $|\psi(t)| \neq \pi/2$ and $\sigma(t) < \infty$. Under these conditions Lemma III.2 shows that ρ and σ converge to their equilibrium state asymptotically. Thus in turn we can conclude from Lemma III.3 that ψ converges to its desired value asymptotically. The convergence of ρ, σ and ψ enables us to use Lemma III.4 to conclude that γ also converges to its equilibrium value. Since Lemma III.1 is true for any initial condition $\bar{Q} \in \bar{D}$, and the convergence of γ is valid for any $\gamma \in \mathcal{S}^1$, we have that any initial condition $q_0 \in D$ asymptotically converges to the equilibrium value for the chosen gains. Thus the equilibrium of (8) is semi-globally asymptotically stable.

REFERENCES

[1] N. Leonard and E. Fiorelli, "Virtual leaders, artificial potentials and coordinated control of groups," in *Decision and Control, 2001. Proceedings of the 40th IEEE Conference on*, vol. 3, 2001, pp. 2968 –2973 vol.3.

[2] J. Desai, J. Ostrowski, and V. Kumar, "Modeling and control of formations of nonholonomic mobile robots," *Robotics and Automation, IEEE Transactions on*, vol. 17, no. 6, pp. 905 –908, dec 2001.

[3] K. Choi, S. Yoo, J. Park, and Y. Choi, "Adaptive formation control in absence of leader's velocity information," *Control Theory Applications, IET*, vol. 4, no. 4, pp. 521 –528, april 2010.

[4] T. Balch and R. Arkin, "Behavior-based formation control for multirobot teams," *Robotics and Automation, IEEE Transactions on*, vol. 14, no. 6, pp. 926 –939, dec 1998.

[5] J. Lawton, R. Beard, and B. Young, "A decentralized approach to formation maneuvers," *Robotics and Automation, IEEE Transactions on*, vol. 19, no. 6, pp. 933 – 941, dec. 2003.

[6] J. Gouvea, A. Pereira, L. Hsu, and F. Lizarralde, "Adaptive formation control of dynamic nonholonomic systems using potential functions," in *American Control Conference (ACC), 2010*, 30 2010-july 2 2010, pp. 230 –235.

[7] M. A. Lewis and K.-H. Tan, "High precision formation control of mobile robots using virtual structures," *Autonomous Robots*, vol. 4, pp. 387–403, 1997, 10.1023/A:1008814708459. [Online]. Available: http://dx.doi.org/10.1023/A:1008814708459

[8] J. Fax and R. Murray, "Information flow and cooperative control of vehicle formations," *Automatic Control, IEEE Transactions on*, vol. 49, no. 9, pp. 1465 – 1476, sept. 2004.

[9] W. Ren, "Consensus based formation control strategies for multi-vehicle systems," in *American Control Conference, 2006*, june 2006, p. 6 pp.

[10] J. Guo, Z. Lin, M. Cao, and G. Yan, "Adaptive leader-follower formation control for autonomous mobile robots," in *American Control Conference (ACC), 2010*, 30 2010-july 2 2010, pp. 6822 –6827.

[11] H. Poonawala, A. Satici, N. Gans, and M. Spong, "Formation control of wheeled robots with vision-based position measurement," in *American Control Conference (ACC), 2012*, june 2012, pp. 3173 –3178.

[12] H. Khalil, *Nonlinear Systems*. Prentice Hall, 2002. [Online]. Available: http://books.google.com/books?id=t_d1QgAACAAJ